

New Limits on the Possible Variation of Physical Constants

M. J. Drinkwater¹, J. K. Webb¹, J. D. Barrow², V. V. Flambaum¹

¹*School of Physics, University of New South Wales, Sydney 2052, Australia*

²*Astronomy Centre, University of Sussex, Brighton, BN1 9QH*

Accepted for publication in MNRAS

ABSTRACT

Recent detections of high-redshift absorption by both atomic hydrogen and molecular gas in the radio spectra of quasars have provided a powerful tool to measure possible temporal and spatial variations of physical ‘constants’ in the Universe.

We have compared the frequency of high-redshift Hydrogen 21 cm absorption with that of associated molecular absorption in two quasars to place new (1 sigma) upper limits on any variation in $y \equiv g_p \alpha^2$ (where α is the fine structure constant and g_p is the proton g-factor) of $|\Delta y/y| < 5 \times 10^{-6}$ at redshifts $z = 0.25$ and $z = 0.68$. These quasars are separated by a comoving distance of 3000 Mpc (for $H_0 = 75 \text{ km s}^{-1} \text{ Mpc}^{-1}$ and $q_0 = 0$). We also derive limits on the time rates of change of $|g_p/g_p| < 1 \times 10^{-15} \text{ y}^{-1}$ and $|\dot{\alpha}/\alpha| < 5 \times 10^{-16} \text{ y}^{-1}$ between the present epoch and $z = 0.68$. These limits are more than an order of magnitude smaller than previous results derived from high-redshift measurements.

Key words: cosmology:observations – ISM:atoms – ISM:molecules – quasars:absorption lines

1 INTRODUCTION

Quasar absorption systems present ideal laboratories in which to search for any temporal or spatial variation in the assumed fundamental constants of Nature. Such ideas date back to the 1930s, with the first constraints from spectroscopy of QSO absorption systems arising in the 1960s. An historical summary of the various propositions is given in Varshalovich & Potekhin (1995) and further discussion of their theoretical consequences is given in Barrow & Tipler (1986).

The subject of varying constants is of particular current interest because of the new possibilities opened up by the structure of unified theories, like string theory and M-theory, which lead us to expect that additional compact dimensions of space may exist. Although these theories do not require traditional constants to vary, they allow a rigorous description of any variations to be provided: one which does not merely ‘write in’ the variation of constants into formulae derived under the assumption that they do not vary. This self-consistency is possible because of the presence of extra dimensions of space in these theories. The ‘constants’ seen in a three-dimensional subspace of the theory will vary at the same rate as any change occurring in the extra compact dimensions. In this way, consistent simultaneous variations of different constants can be described and searches for varying constants provide a possible observational handle on the question of whether extra dimensions exist (Marciano 1984, Barrow 1987, Damour & Polyakov 1994).

Prior to the advent of theories of this sort only the time variation of the gravitational constant could be consistently described using scalar-tensor gravity theories, of which the Brans-Dicke theory is the simplest example. The modeling of variations in other ‘constants’ was invariably carried out by assuming that the time variation of a constant quantity, like the fine structure constant, could just be written into the usual formulae that hold when it is constant. The possibility of linked variations in low-energy constants as a result of high-energy unification schemes has the added attraction of providing a more powerful means of testing those theories (Marciano 1984, Kolb, Perry & Walker 1986, Barrow 1987, Dixit & Sher 1988, Campbell & Olive 1995).

Higher-dimensional theories typically give rise to relationships of the following sort

$$\begin{aligned} \alpha_i(m_*) &= A_i G m_*^2 = B_i \lambda^n (\ell_{pl}/R)^m; n, m \text{ constants} \quad (1) \\ \alpha_i^{-1}(\mu) &= \alpha_i^{-1}(m_*) - \\ &\pi^{-1} \sum C_{ij} [\ln(m_*/m_j) + \theta(\mu - m_j) \ln(m_j/\mu)] + \Delta_i \end{aligned}$$

where $\alpha_i(\dots)$ are the three gauge couplings evaluated at the corresponding mass scale; μ is an arbitrary reference mass scale, m_* is a characteristic mass scale defining the theory (for example, the string scale in a heterotic string theory); λ is some dimensionless string coupling; $\ell_{pl} = G^{-1/2}$ is the Planck length, and R is a characteristic mean radius of the compact extra-dimensional manifold; C_{ij} are numbers defined by the particular theories and the constants A_i and B_i depend upon the topology of the additional (> 3) dimen-

arXiv:astro-ph/9711290v1 25 Nov 1997

sions. The sum is over $j = \text{leptons, quarks, gluons, } W^\pm, Z$ and applies at energies above $\mu \sim 1 \text{ GeV}$ (Marciano 1984). The term Δ_i corresponds to some collection of string threshold corrections that arise in particular string theories or an over-arching M theory (Antoniadis & Quiros 1997). They contain geometrical and topological factors which are specified by the choice of theory. By differentiating these two expressions with respect to time (or space), it is possible to determine the range of self-consistent variations that are allowed. In general, for a wide range of supersymmetric unified theories, the time variation of different low-energy constants will be linked by a relationship of the form (where we consider $\dot{\beta}$ to denote the time derivative of β etc.)

$$\delta_0 \frac{\dot{\beta}}{\beta} = \delta_1 \frac{\dot{G}}{G} + \sum \delta_{2i} \frac{\dot{\alpha}_i}{\alpha_i^2} + \delta_3 \frac{\dot{m}_*}{m_*} + \sum \delta_{4j} \frac{\dot{m}_j}{m_j} + \delta_5 \frac{\dot{\lambda}}{\lambda} + \dots (2)$$

where $\beta \equiv m_e/m_p$ is the electron-proton mass ratio. It is natural to expect that all the terms involving time derivatives of ‘constants’ will appear in this relation unless the constant δ prefactors vanish because of supersymmetry or some other special symmetry of the underlying theory. This relation shows that, since we might expect all terms to be of similar order (although there may be vanishing constant δ prefactors in particular theories), we might expect variations in the Newtonian gravitational ‘constant’, \dot{G}/G , to be of order $\dot{\alpha}/\alpha^2$.

In this paper, we consider only the bounds that can be placed on the variation of the fine structure constant and proton g factor from radio observations of atomic and molecular transitions in high redshift quasars. To do this we exploit the recent dramatic increase in quality of spectroscopic molecular absorption at radio frequencies, of gas clouds at intermediate redshift, seen against background radio-loud quasars. Elsewhere, we will consider the implications of simultaneous variations of several ‘constants’ and show how these observational limits can be used to constrain a class of inflationary universe theories in which small fluctuations in the fine-structure constant are predicted to occur.

The rotational transition frequencies of diatomic molecules such as CO are proportional to $\hbar/(Ma^2)$ where M is the reduced mass and $a = \hbar^2/(m_e e^2)$ is the Bohr radius. The 21 cm hyperfine transition in hydrogen has a frequency proportional to $\mu_p \mu_B / (\hbar a^3)$, where $\mu_p = g_p e \hbar / (4m_p c)$, g_p is the proton g -factor and $\mu_B = e \hbar / (2m_e c)$. Consequently (the dependence of the results on the proton-neutron mass difference $m_p - m_n$ is very small so we assume m_p/M is constant) the ratio of a hyperfine frequency to a molecular rotational frequency is proportional to $g_p \alpha^2$ where $\alpha = e^2/(\hbar c)$ is the fine structure constant. Any variation in $y \equiv g_p \alpha^2$ would therefore be observed as a difference in the apparent redshifts: $\Delta z/(1+z) \approx \Delta y/y$. Redshifted molecular emission is hard to detect but absorption can be detected to quite high redshifts (see review by Combes & Wiklind 1996). Recent measurements of molecular absorption in some radio sources corresponding to known HI 21 cm absorption systems give us the necessary combination to measure this ratio at different epochs.

Common molecular and HI 21 cm absorptions in the radio source PKS 1413+135 have previously been studied by Varshalovich & Potekhin (1996). They reported a difference in the redshifts of the CO molecular and HI 21 cm atomic absorptions which they interpreted as a mass change

Table 1. Sources with Galactic Absorption

Name	NED Name	l deg	b deg
0212+735	[HB89] 0212+735	128.93	11.96
0224+671	4C +67.05	132.12	6.23
0355+508	4C +50.11	150.38	-1.60
0415+379	3C111	161.68	-8.82
0727-115	PKS 0727-11	227.77	3.14
1730-130	[HB89] 1730-130	12.03	10.81
2013+370	[CCS92] 2013+370	74.87	1.22
2037+511	[HB89] 2037+511	88.81	6.04
2200+420	[HB89] 2200+420	92.59	-10.44

Note: ‘NED Name’ gives names under which the sources are recorded in the NASA/IPAC Extragalactic Database.

of $\Delta M/M = (-4 \pm 6) \times 10^{-5}$ but as we show above this comparison actually constrains $g_p \alpha^2$, not mass. Furthermore they used overestimates of both the value and error. They used the Wiklind & Combes (1994) measurement which had the CO line offset from the HI velocity by -11 km s^{-1} ; a corrected CO measurement (Combes & Wiklind 1996) shows there is no measurable offset. Furthermore Varshalovich & Potekhin (1996) used the width of the HI line for the measurement uncertainty. Even allowing for systematic errors the true uncertainty is at least a factor of 10 smaller so these data in fact establish a limit of order 10^{-5} or better. This potential for improved limits has prompted the present investigation: previous upper limits on change in α are of order $\Delta\alpha/\alpha \approx 10^{-4}$ (Cowie & Songalia 1995; Varshalovich, Panchuk & Ivanchik 1996).

We consider three sources for which combined HI 21 cm and molecular absorption detections have now been published. Before examining them in detail we look at some examples of local Galactic absorption in Section 2 to show that the same clouds are detected in both atomic and molecular absorption. In Section 3 we summarize the published measurements of the sources and reanalyze the HI data with smaller errors than Varshalovich & Potekhin (1996) to obtain improved upper limits on the variation of $g_p \alpha^2$. The interpretations of the results, a comparison with terrestrial limits, and future prospects are described in Section 4.

2 SOURCES WITH GALACTIC ABSORPTION

One possible problem with this approach is that the HI and molecular absorptions might result from different clouds along the respective lines of sight. We need to show that if we take the nearest HI system closest in velocity to a given molecular absorption they are associated and not just a random superposition of different absorbing clouds. We investigated this by looking at a sample of extragalactic mm-wave continuum sources (Liszt & Lucas 1996). Nine of these sources have both HCO⁺ absorption measured by Liszt & Lucas and HI absorption measured by Dickey et al. (1983). We note that these sources are all at low Galactic latitude and will therefore experience more absorption than we would expect from extragalactic sources intersecting randomly oriented external galaxies.

The nine Liszt & Lucas sources with both HI and HCO⁺ absorption are listed in Table 1 and we plot their HI spectra

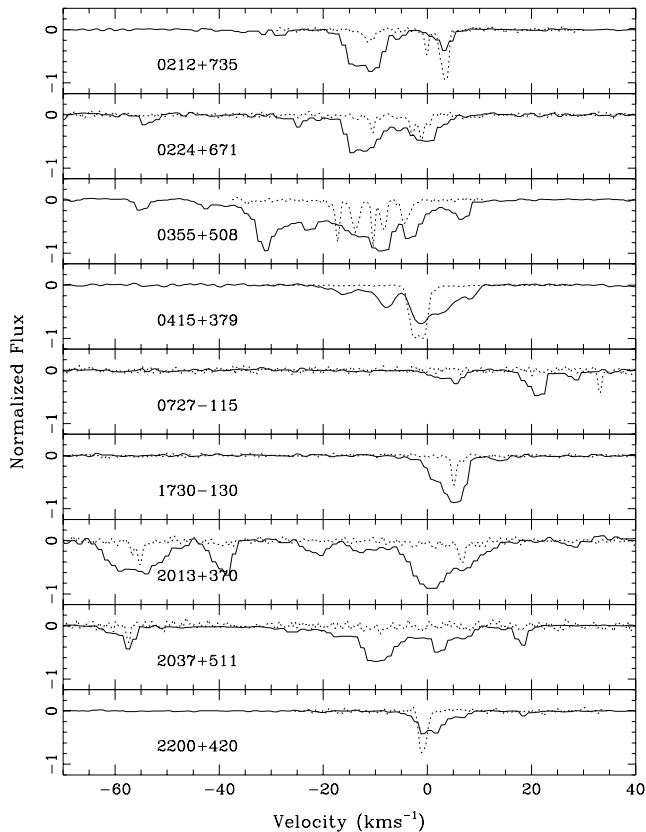


Figure 1. HI and HCO⁺ spectra of sources with Galactic absorption. The HI data (solid lines) are from Dickey et al. (1983) and the HCO⁺ data (dotted lines) are from Liszt & Lucas (1996). The velocity scale is with respect to the rest frequency of the respective lines in the local standard of rest frame.

with the HCO⁺ overlaid in Fig. 1 using data kindly provided by the respective authors. They are plotted on common velocity scales with respect to the rest frequency f_{rest} of the corresponding transition at the local standard of rest frame. The velocities v are approximated from the observed frequency f_{obs} by $v/c = 1 - f_{obs}/f_{rest}$ where c is the speed of light.

The velocity structure of the HI absorption is complex in most of the sources, consistent with the low Galactic latitudes of these lines of sight. The tendency for most absorption to be at negative velocities (as illustrated in Fig. 1) is a consequence of Galactic rotation and the Galactic longitudes of the sources.

Although these lines of sight display many more HI absorption systems than for HCO⁺, our aim is just to test the hypothesis that every molecular absorption can be directly associated with HI at the closest velocity: to do this we fitted velocity components to the HI and molecular data independently and then compared the velocity differences statistically.

The procedure adopted for fitting was as follows. As described above, we treated the HI and HCO⁺ data independently, so we did not require the same numbers of components in both HI and HCO⁺ systems. We used the VP-

Table 2. New HI absorption line fits

Name	z_{ref}	z_{obs}	offset (km s^{-1})	ID
0218+357	.684680 ¹	.684495±.000010	-32.9±1.8	1
“	“	.684568±.000011	-20.0±1.9	2
“	“	.684684±.000006	0.8±1.0	3*
1413+135	.246710 ²	.246710±.000004	0.0±0.9	1*
“	“	.246770±.000037	14.5±8.8	2
1504+377	.671500 ³	.673015±.000014	271.6±2.5	1
“	“	.673236±.000003	311.2±0.5	2*
“	“	.673423±.000005	344.7±0.8	3*
“	“	.673569±.000068	370.8±12	4

Notes: z_{obs} is the fitted redshift and uncertainty including both fitting and velocity scale (0.3 km s^{-1}) errors; offset is the velocity of the fitted line with respect to the reference redshift z_{ref} taken from the references listed in Table 3. ID is the number of the component labeled in Fig. 3 with an * to indicate the strongest lines used to compare with the molecular data.

FIT software (Webb 1987) to fit multiple components to both the HI and HCO⁺ absorption systems. VPFIT uses an unconstrained non-linear least-squares optimization method to fit Gaussian/Voigt profiles to the absorption lines in each system. We adopted the standard approach of fitting the minimum number of components required to obtain a statistically acceptable fit, i.e. that the normalized χ^2 was close to unity. The fitting process was also constrained not to introduce any components narrower than the instrumental resolution.

The results of the fitting process are summarized in Fig. 2, a histogram of the (HI - HCO⁺) velocity differences for all systems (solid line) and the closest matching pairs (dashed line). The distribution of all pairs shows a peak at zero; it is also skewed to negative velocities because HI is detected out to larger Galactocentric distances than HCO⁺.

To test our hypothesis of a physical association between each molecular system and the HI component closest to it in velocity, we show in Fig. 2 the histogram of closest (nearest-neighbour) velocity differences. This distribution is centred close to zero (mean $\Delta v = 0.4 \text{ km s}^{-1}$) and is very narrow with a Gaussian dispersion of only 1.2 km s^{-1} . This is equal to the spectral resolution of the HI data ($0.6\text{--}1.3 \text{ km s}^{-1}$) (Liszt & Lucas 1996). To show that the narrow distribution of the nearest velocities is significant and does not result from choosing nearest pairs from uncorrelated spectra we also plot in Fig. 2 the distribution of nearest lines (dotted line) where, for each source, we replaced all the HI velocities by a random selection of HI lines from all the other sources. This shows no peak at zero so we conclude that the absorption is from the same clouds to within our velocity resolution.

3 HIGH-REDSHIFT ABSORPTION SYSTEMS

3.1 Sample of redshifted absorbers

We found three sources with common extragalactic molecular and HI absorption detections published: 0218+357,

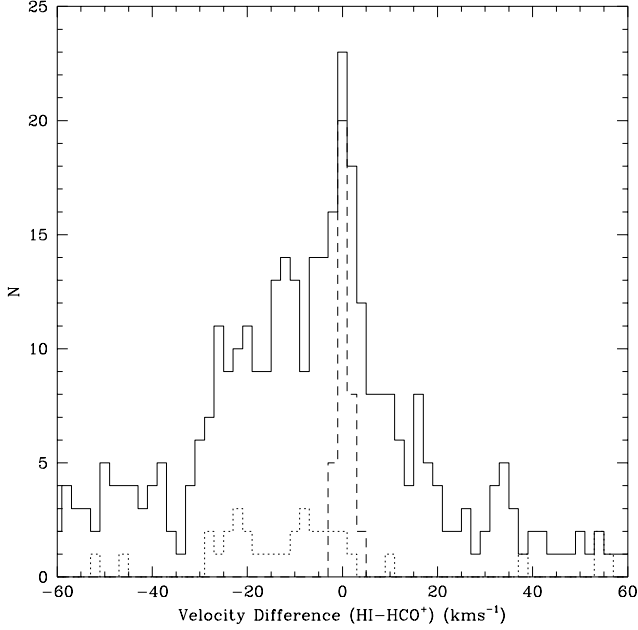


Figure 2. Histogram of the HI – HCO⁺ velocity differences for all the sources with Galactic absorption listed above. For each source all line pair differences were used to give the solid histogram. The dashed line indicates the nearest HI to each HCO⁺ line. The dotted line is the result of a random simulation of the nearest pair data to show that the peak for the nearest lines is real.

1413+135 and 1504+377. The details of these sources are listed below in Table 3. The sources include 1413+135 which was previously discussed by Varshalovich & Potekhin (1996). The published HI data are also included in Table 3. The typical HI error of $\Delta z/(1+z) = 1 \times 10^{-5}$ (3 km s^{-1}) is smaller than the value used by Varshalovich & Potekhin (1996), but still the dominant term. We show in the next section how we improved the HI precision by refitting HI lines to the data kindly provided by Dr. C. Carilli. We then compared these to the published molecular data to put new limits on the variation of $g_p \alpha^2$.

3.2 HI absorption systems

In this section we describe how we obtained more precise redshifts for the HI absorption data. A good rule of thumb is that the uncertainty in fitting a line position is about one tenth of a resolution element. In the case of the HI data for 1504+377 the resolution was 10 kHz per channel at 848.8 MHz or about 3 km s^{-1} , about the error quoted by Carilli et al. (1997). Applying the one tenth of a channel criterion we might expect to better than this, although we must also consider any systematic errors. Checks made by Carilli et al. (1997) indicate that the systematic errors in the velocity scale are about 0.8 kHz or 0.3 km s^{-1} .

The HI data for three sources are shown plotted in Fig. 3. We used the VPFIT software described above to decompose the absorption systems, following the same procedure as before, fitting a number of components to each system. The resulting fits are plotted over the data in Fig. 3.

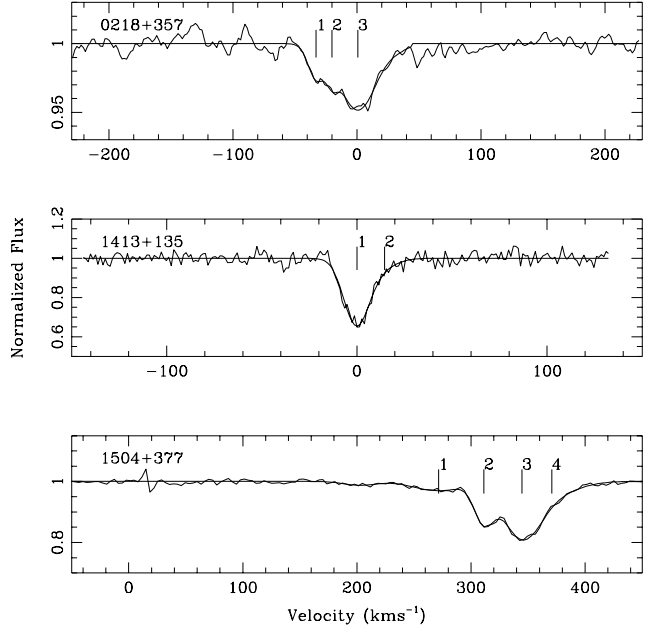


Figure 3. Spectra of three quasars with high-redshift HI absorption. The data are from references 2, 4 and 6 listed in Table 3. The velocity zero points are taken from the same references. The spectra were first normalized to a continuum of unity and then deconvolved by fitting multiple absorption components as described in the text: the final fit is plotted over the data as a continuous smooth line with the centres of each component marked.

All the components we fitted to each source are listed in Table 2, both in terms of observed redshift and a velocity offset with respect to the nominal redshift. The fitting routine gave uncertainties less than 1 km s^{-1} for the strong lines; these were added in quadrature with the velocity scale uncertainty of 0.3 km s^{-1} to obtain the errors given in Table 2.

As with the low redshift galactic absorption we took the nearest matches between these HI absorption detections and the molecular absorption redshifts listed in Table 3.

3.3 Molecular absorption systems

The redshifts of the molecular absorptions are listed in Table 3. These are—in principle—much more precise than the HI data, with velocity uncertainties of 0.1 km s^{-1} . In practice, the published values were not quoted to this precision because they were not aimed at this kind of work. We have taken the best estimates of the molecular redshifts and uncertainties from the publications as follows.

In the case of 0218+357 Wiklind & Combes (1995) work with respect to the HI redshift of $z = 0.68466$ (Carilli, Rupen & Yanny 1993) but it is clear from their Fig. 3 that the centre of the molecular absorption (measured from the HCO⁺ system) is $4 \pm 0.5 \text{ km s}^{-1}$ higher corresponding to $z = 0.684680 \pm 0.000006$, the value we adopt here.

The velocity of the CO absorption in 1413+135 was originally found to be offset from the HI result by Wiklind & Combes (1994) but this was subsequently corrected and is equal to the HI value of $z=0.24671$ (Combes & Wiklind 1996). We assume the uncertainty in the molecular redshift

Table 3. Comparison of Molecular and Atomic Absorption Data

Name	NED Name	Molecular z	Molecule	Atomic z (HI)	Atomic z (HI, new)	$\sigma_{\Delta z/1+z}$
0218+357	TXS 0218+357	0.684680 ± 0.000006^1	HCO ⁺ (2-1)	0.68466 ± 0.00004^2	0.684684 ± 0.000006	5×10^{-6}
1413+135	PKS 1413+135	0.246710 ± 0.000005^3	CO(0-1)	0.24671 ± 0.00001^4	0.246710 ± 0.000004	5×10^{-6}
1504+377	B3 1504+377	0.673350 ± 0.000005^5	HCO ⁺ (2-1)	0.67324 ± 0.00001^6	0.673236 ± 0.000003	–
1504+377	“	0.673350 ± 0.000005^5	HCO ⁺ (2-1)	0.67343 ± 0.00001^6	0.673423 ± 0.000005	–

References:

- 1: Wiklind & Combes (1995) modified; see text,
- 2: Carilli, Rupen & Yanny (1993),
- 3: Wiklind & Combes (1994) corrected by Combes & Wiklind (1996),
- 4: Carilli, Perlman & Stocke (1992),
- 5: Wiklind & Combes (1996),
- 6: Carilli et al. (1997).

is half the least significant digit, although the potential value is much smaller.

The redshift of the molecular absorption in 1504+377 quoted by Wiklind & Combes (1996) ($z=0.67335$) is not consistent with the HI detections of (Carilli et al. 1997). Carilli et al. interpret this difference as either a shift of 15 km s^{-1} in one of the velocity scales or intrinsic differences in the atomic and molecular absorption. Their HI redshift has been confirmed by subsequent independent observations (Carilli et al. 1998, Ap.J., submitted). Our own deconvolution of the HI data gives a 4-line system very similar to, but displaced by a constant shift from, the HCO⁺ absorption data in Fig. 2(a) of Wiklind & Combes (1996). An offset of a single line could be interpreted as a case of different clouds causing the absorption, but a systematic offset of 4 lines is much more likely due to a velocity error in one of the measurements. We have not used 1504+377 in our analysis below because of this disagreement.

3.4 Comparison of HI and molecular systems

Our new more accurate redshift estimates are listed with the molecular results in Table 3. In the two sources 0218+357 and 1413+135 the redshifts agree to within our errors. (As discussed above we are not analyzing 1504+377.) We can therefore combine the uncertainties in quadrature to give 1-sigma upper limits on the redshift differences. These are shown in the Table and are $|\Delta z/1+z| < 5 \times 10^{-6}$ (1.5 km s^{-1}) for both sources.

We must still consider the possibility that the molecular and atomic absorption arises in different gas clouds along the line of sight. This could explain any observed difference. However there is no measurable difference between the two velocities in our data, so we are probably detecting the same gas. The alternative would be that there was a change in the frequencies but that in both cases it was exactly balanced by the random relative velocity of the two gas clouds observed. We consider this very unlikely because of the small 1 km s^{-1} dispersion within single clouds shown in Section 2.

4 DISCUSSION

We can now use the limits to $\Delta z/1+z$ with the relationship given in Section 1 to derive 1-sigma limits on any change in $y = g_p \alpha^2$: $|\Delta y/y| < 5 \times 10^{-6}$ at both $z = 0.25$ and $z = 0.68$.

These are significantly lower than the previous best limit of 1×10^{-4} by Varshalovich & Potekhin (1996) (it was quoted as a limit on nucleon mass, but it actually refers to $g_p \alpha^2$).

As there are no theoretical grounds to expect that the changes in g_p and α^2 are inversely proportional, we obtain independent rate-of-change limits of $|g_p/g_p| < 2 \times 10^{-15} \text{ y}^{-1}$ and $|\dot{\alpha}/\alpha| < 1 \times 10^{-15} \text{ y}^{-1}$ at $z = 0.25$ and $|g_p/g_p| < 1 \times 10^{-15} \text{ y}^{-1}$ and $|\dot{\alpha}/\alpha| < 5 \times 10^{-16} \text{ y}^{-1}$ at $z = 0.68$ (for $H_0 = 75 \text{ km s}^{-1} \text{ Mpc}^{-1}$ as adopted throughout this section). These new limits are much lower than the previous 1 sigma limit of $|\dot{\alpha}/\alpha| < 8 \times 10^{-15} \text{ y}^{-1}$ at $z \approx 3$ (Varshalovich et al. 1996).

The most stringent laboratory bound on the time variation of α comes from a comparison of hyperfine transitions in Hydrogen and Mercury atoms (Prestage, Tjoelker & Maleki 1995), $|\dot{\alpha}/\alpha| < 3.7 \times 10^{-14} \text{ y}^{-1}$, and is significantly weaker than our astronomical limit. The other strong terrestrial limit that we have on time variation in α comes from the analysis of the Oklo natural reactor at the present site of an open-pit Uranium mine in Gabon, West Africa. A distinctive thermal neutron capture resonance must have been in place 1.8 billion years ago when a combination of fortuitous geological conditions enriched the subterranean Uranium-235 and water concentrations to levels that enabled spontaneous nuclear chain reactions to occur (Maurette 1972). Shlyakhter (1976, 1983) used this evidence to conclude that the neutron resonance could not have shifted from its present specification by more than $5 \times 10^{-4} \text{ eV}$ over the last 1.8 billion years and, assuming a simple model for the dependence of this energy level on coupling constants like α , derived a limit in the range of $|\dot{\alpha}/\alpha| < (0.5-1.0) \times 10^{-17} \text{ y}^{-1}$. The chain of reasoning leading to this very strong bound is long, and involves many assumptions about the local conditions at the time when the natural reactor ran, together with modeling of the effects of any variations in electromagnetic, weak, and strong couplings. Recently, Damour & Dyson (1997) have provided a detailed reanalysis in order to place this limit on a more secure foundation. They weaken Shlyakhter's limits slightly but give a 95% confidence limit of $-6.7 \times 10^{-17} \text{ y}^{-1} < \dot{\alpha}/\alpha < 5.0 \times 10^{-17} \text{ y}^{-1}$. However, if there exist simultaneous variations in the electron-proton mass ratio this limit can be weakened.

The Oklo results provide stronger limits on the time variation of α than the astronomical data; however, the astronomical limits have the distinct advantage of resting upon a very short chain of theoretical deduction and are

more closely linked to repeatable precision measurements of a simple environment. The Oklo environment is sufficiently complex for significant uncertainties to remain.

Unlike the Oklo limits, the astronomical limits also allow us to derive upper limits on any *spatial* variation in α . Spatial variation is expected from the theoretical result that the values of the constants would depend on local conditions and that they would therefore vary in both time and space (Damour & Polyakov 1994). The two sources for which we derived limits, 0218+357 and 1413+135, are separated by 131 degrees on the sky, so together with the terrestrial result, we find the same values of α to within $|\Delta\alpha/\alpha| < 3 \times 10^{-6}$ in three distinct regions of the universe separated by comoving separations up to 3000 Mpc. Limits on spatial variation of $g_p\alpha^2 m_e/m_p$ were previously discussed by Pagel (1977, 1983) and Tubbs & Wolfe (1980). We have improved on their limits by some 2 orders of magnitude but as our sources are at lower redshift, they are not causally disjoint from each other.

With a careful reanalysis of the available data we have made a significant improvement on the existing upper limits on any change of the product of two physical constants $g_p\alpha^2$ with cosmic time. The high-redshift measurements are now approaching the best terrestrial measurements based on the Oklo data. These could be further improved by a factor of 2–5 with additional observations that would not be difficult to perform such as fitting the atomic and molecular data simultaneously, remeasuring the HI absorptions at higher spectral resolution, and checking the discrepancy in the observations of 1504+377.

ACKNOWLEDGMENTS

We are very grateful Drs. C. Carilli, H. Liszt, and J. Dickey for many helpful discussions and for allowing us to use their data. We also wish to thank Drs. F. Combes, T. Wiklind and A. Potekhin for helpful comments about this work. The referee of this paper also made a number of suggestions that greatly improved the presentation of these results. We used the NASA/IPAC Extragalactic Database (NED) which is operated by the Jet Propulsion Laboratory, Caltech, under contract with the National Aeronautics and Space Administration.

REFERENCES

- Antoniadis, I., Quiros, M., 1997, *Phys. Lett.*, B392, 61
 Barrow, J. D., 1987, *Phys. Rev.*, D35, 1805
 Barrow, J. D., Tipler, F. J., 1986, *The Anthropic Cosmological Principle*. Oxford Univ. Press, Oxford, p. 533
 Campbell, B. A., Olive, K. A., 1995, *Phys. Lett.*, B345, 429
 Carilli, C. L., Perlman, E. S., Stocke, J. T., 1992, *ApJ*, 400, L13
 Carilli, C. L., Rupen, M. P., Yanny, B., 1993, *ApJ*, 412, L59
 Carilli, C. L., Menten, K. M., Reid, M. J., Rupen, M. P., 1997, *ApJ*, 474, L89
 Combes, F., Wiklind, T., 1996, in Bremer, M., van der Werf, P., Rottgering, H., Carilli, C., eds, *Cold Gas at High Redshift*. Kluwer, Dordrecht, p. 215
 Cowie, L. L., Songalia, A., 1995, *ApJ*, 453, 596

- Damour, T., Dyson, F., 1997, *Nucl. Phys.*, B480, 37
 Damour, T., Polyakov, A. M., 1994, *Nucl. Phys.*, B423, 596
 Dickey, J. E., Kulkarni, S. R., van Gorkom, J. H., Heiles, C. E., 1983, *ApJS*, 53, 591
 Dixit, V. V., Sher, M., 1988, *Phys. Rev.*, D37, 1097
 Kolb, E. W., Perry, M. J., Walker, T. P., 1986, *Phys. Rev.*, D33, 869
 Liszt, H., Lucas, R., 1996, *A&A*, 314, 917
 Marciano, W., 1984 *Phys. Rev. Lett.*, 52, 489
 Maurette, M., 1972, *Ann. Rev. Nucl. Part. Sci.*, 26, 319
 Pagel, B. E. J., 1977, *MNRAS* 179, 81P
 Pagel, B. E. J., 1983, *Phil. Trans. Roy. Soc.*, A310, 245
 Prestage, J. D., Tjoelker, R. L., Maleki, L., 1995, *Phys. Rev. Lett.*, 74, 3511
 Shlyakhter, A. I., 1976, *Nature*, 264, 340
 Shlyakhter, A. I., 1983, Direct test of the time-independence of fundamental nuclear constants using the Oklo natural reactor, ATOMKI Report A/1
 Tubbs, A. D., Wolfe, A. M., 1980, *ApJ*, 236, L105
 Varshalovich, D. A., Potekhin, A. Y., 1995, *Space Science Review*, 74, 259
 Varshalovich, D. A., Potekhin, A. Y., 1996, *Pis'ma Astron. Zh.*, 22, 3
 Varshalovich, D. A., Panchuk, V. E., Ivanchik, A. V., 1996, *Astron. Lett.*, 22, 6
 Webb, J. K., 1987, PhD thesis, University of Cambridge
 Wiklind, T., Combes, F., 1994, *A&A*, 286, L9
 Wiklind, T., Combes, F., 1995, *A&A*, 299, 382
 Wiklind, T., Combes, F., 1996, *A&A*, 315, 86